

Accepted Manuscript

Synthesis and anti-cancer evaluation of folic acid-peptide- paclitaxel conjugates for addressing drug resistance

Yuxuan Dai, Xingguang Cai, Xinzhou Bi, Chunxia Liu, Na Yue, Ying Zhu, Jiaqi Zhou, Mian Fu, Wenlong Huang, Hai Qian



PII: S0223-5234(19)30249-1

DOI: <https://doi.org/10.1016/j.ejmech.2019.03.031>

Reference: EJMECH 11201

To appear in: *European Journal of Medicinal Chemistry*

Received Date: 10 December 2018

Revised Date: 13 March 2019

Accepted Date: 13 March 2019

Please cite this article as: Y. Dai, X. Cai, X. Bi, C. Liu, N. Yue, Y. Zhu, J. Zhou, M. Fu, W. Huang, H. Qian, Synthesis and anti-cancer evaluation of folic acid-peptide- paclitaxel conjugates for addressing drug resistance, *European Journal of Medicinal Chemistry* (2019), doi: <https://doi.org/10.1016/j.ejmech.2019.03.031>.

This is a PDF file of an unedited manuscript that has been accepted for publication. As a service to our customers we are providing this early version of the manuscript. The manuscript will undergo copyediting, typesetting, and review of the resulting proof before it is published in its final form. Please note that during the production process errors may be discovered which could affect the content, and all legal disclaimers that apply to the journal pertain.

Graphical Abstract for

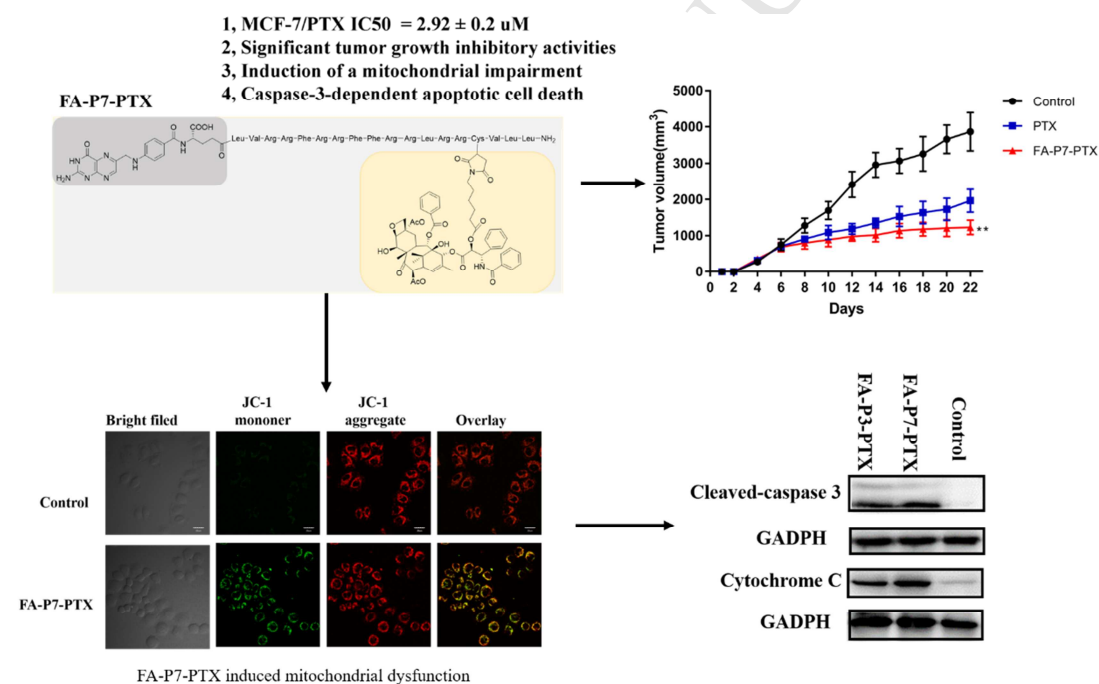
Synthesis and anti-cancer evaluation of folic acid-peptide- paclitaxel conjugates for addressing drug resistance

Yuxuan Dai ^a, Xingguang Cai ^a, Xinzhou Bi ^a, Chunxia Liu ^a, Na Yue ^a, Ying Zhu ^a, Jiaqi Zhou ^a, Mian Fu ^{a, b}, Wenlong Huang ^{a, c}, Hai Qian ^{a, c*}

^a Center of Drug Discovery, State Key Laboratory of Natural Medicines, China Pharmaceutical University, 24 Tongjiaxiang, Nanjing 210009, PR China

^b Department of Biochemistry and Molecular Biology, Nanjing Medical University, 140 Hanzhong Road, Nanjing 210029, PR China.

^c Jiangsu Key Laboratory of Drug Discovery for Metabolic Disease, China Pharmaceutical University, 24 Tongjiaxiang, Nanjing 210009, PR China



* Corresponding author: Hai Qian, Centre of Drug Discovery, State Key Laboratory of Natural Medicines, China Pharmaceutical University, 24 Tongjiaxiang, Nanjing 210009, China.

Tel: +86-25-83271051; Fax: +86-25-83271051.

E-mail: qianhai24@163.com (H. Qian).

Synthesis and anti-cancer evaluation of folic acid-peptide-paclitaxel conjugates for addressing drug resistance

Yuxuan Dai ^a, Xingguang Cai ^a, Xinzhou Bi ^a, Chunxia Liu ^a, Na Yue ^a, Ying Zhu ^a, Jiaqi Zhou ^a, Mian Fu ^{a, b}, Wenlong Huang ^{a, c}, Hai Qian ^{a, c*}

^a Center of Drug Discovery, State Key Laboratory of Natural Medicines, China Pharmaceutical University, 24 Tongjiaxiang, Nanjing 210009, PR China

^b Department of Biochemistry and Molecular Biology, Nanjing Medical University, 140 Hanzhong Road, Nanjing 210029, PR China.

^c Jiangsu Key Laboratory of Drug Discovery for Metabolic Disease, China Pharmaceutical University, 24 Tongjiaxiang, Nanjing 210009, PR China

Abstract

The drug resistance and the poor water solubility are major limitations of paclitaxel (PTX) of based chemotherapy. To conquer the two problems, targeting folate (FA) receptor PTX-lytic peptides conjugates were synthesized and evaluated. Compared with PTX, FA-P3-PTX and FA-P7-PTX displayed significantly enhanced cell toxicity in many cancer cells, particularly drug resistant cancer cells MCF-7/PTX.

FA-P7-PTX possessed stronger effect on cell toxicity ($IC_{50} = 2.92 \pm 0.2 \mu M$), membrane disrupting activity and pro-apoptosis in MCF-7/PTX cells than FA-P3-PTX. Further investigation displayed that the anti-cancer mechanisms of FA-P3-PTX and FA-P7-PTX might be a mitochondrial impairment and caspase-3-dependent apoptotic cell death. Furthermore, the *in vivo* antitumor efficacy study confirmed that FA-P7-PTX performed more stronger potency in inhibition of

* Corresponding author: Hai Qian, Centre of Drug Discovery, State Key Laboratory of Natural Medicines, China Pharmaceutical University, 24 Tongjiaxiang, Nanjing 210009, China.

Tel: +86-25-83271051; Fax: +86-25-83271051.

E-mail: qianhai24@163.com (H. Qian).

tumors growth than PTX.

The study demonstrated that conjugate FA-P7-PTX with superior properties for antineoplastic activity, which makes it a promising potential candidate for drug-resistant cancer therapy.

Keywords

Lytic peptides, Folate receptor targeted, Membranolytic, Apoptosis, Drug resistance, Paclitaxel, Conjugates of paclitaxel

1. Introduction

Cancer is a leading cause of morbidity and mortality globally, and is responsible for an estimated 9.6 million deaths in 2018¹. Chemotherapy is an important approach used in cancer therapy, while the development of multidrug resistance (MDR)² is a major cause of failure in cancer treatment³. The most common mechanism of cancer MDR is the overexpression of energy-dependent efflux pumps such as P-glycoprotein, a main member of adenosine triphosphate-binding cassette (ABC) transporters⁴⁻⁵. Consequently, it is imperative to develop alternative new potent and less toxic chemotherapeutic agents.

Paclitaxel (PTX)⁶ is a potent anticancer agent frequently used for treatment of a wide variety of human malignancies such as breast, ovarian, lung, and other cancers⁶⁻⁷. However, the application of PTX was limited due to its poor aqueous solubility⁸, systematic toxicity and acquired drug resistant⁹. As a substrate of P-glycoprotein¹⁰, antitumor efficacy of PTX is reduced considerably owing to MDR¹¹⁻¹². The initial formulation of paclitaxel was Cremophor EL- paclitaxel (CrEL-paclitaxel)¹³, the widely used formulation in the clinical setting¹⁴. But, due to its undesirable toxicity, many formulations have already been developed to ameliorate systematic toxicity, such as Lipusu (liposomal PTX), Abraxane (PTX nanoparticles)¹⁵, Genexol-PM¹⁶

(polymer micelles)¹⁶⁻¹⁷, and NK105 (a PTX-incorporating micellar nanoparticle)¹⁸. Compared to PTX, these formulations reduced systematic toxicity and improved water solubility, however, they are not efficient for MDR tumor.

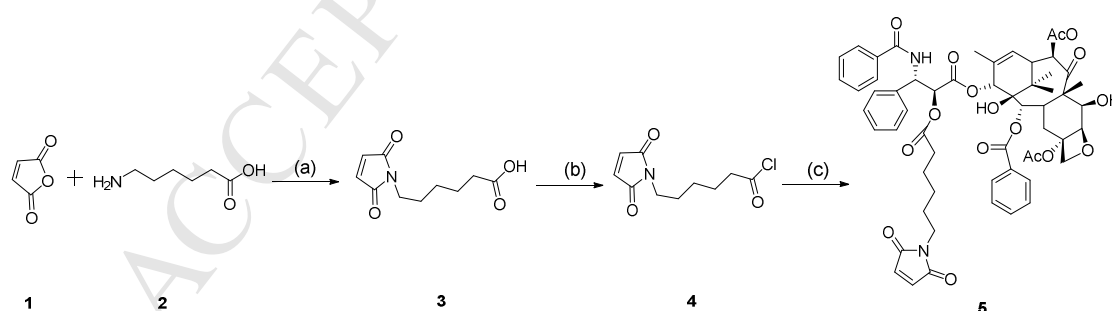
Peptide carrier-mediated drug delivery has been used as a powerful strategy to increase the drug's water solubility¹⁹, optimize to improve cellular uptake²⁰, to achieve cell penetration or selectivity²¹, and to reduce the side effects of cytotoxic drugs²². Meanwhile, peptide mediated drug delivery system, as one of the main pillars, is applied to overcome MDR^{11, 23}. Many researchers have put their mind to constructing new antitumor drug conjugates to solve the drug resistance of tumors²⁴. For instance, Sheng et al. designed a peptide-DOX conjugate and successfully used it to reverse the drug resistance of breast cancer cells²⁵. Lytic peptides, consist of basic amino acids and about half hydrophobic amino acids, are cationic and amphipathic²⁶, which could arrange into amphipathic structure and display potent cell penetration and disruption of cell membrane²⁷. The tumor cell membranes comprise a high proportion of net negative charges so that the cationic lytic peptides could selectively bind with tumor cells by the electrostatic interactions²⁸⁻²⁹. Accordingly, lytic peptides could be used as efficient tools for delivering pharmaceuticals into cells. The strategy that conjugate PTX to lytic peptide can inhibit drug resistance by enhancing the transport PTX into tumor cells, as well as improving water solubility to avoid the use of Cremophor EL.

Folate (FA) receptors are attractive molecular targets for anticancer drug delivery^{30, 31}, which are characteristically overexpressed in many solid tumors including breast³², hepatic carcinoma and others³³, while its expression is low in normal tissues³¹. Folate conjugation offers some functional roles, namely, selective delivery of nonspecific drugs into cancer cells³⁴, reducing adverse side effects on health cells and facilitating cell internalization via receptor-mediated endocytosis³⁵. For example, vintafolide, a folate-conjugated vinca alkaloid desacetylvinblastine hydrazide, is currently undergoing phase II clinical studies in patients with platinum-resistant ovarian cancer³⁶ and non-small cell lung cancer³⁷.

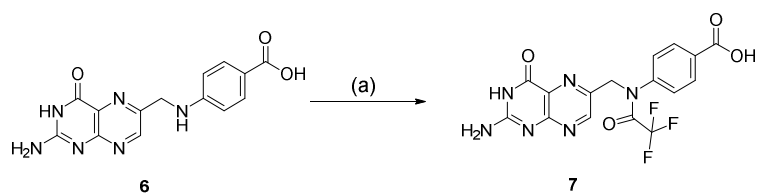
We have previously reported that structural optimized lytic peptides I-3 and I-7 can be used as cell-disrupting peptides and molecular carriers³⁸. Meanwhile, PTX, a firstline antitumor drug, its poor aqueous solubility (no more than 0.004 mg/mL)⁸ and acquired drug resistant need to be addressed urgently. In this work, we choose the 16-site cysteine-substituted I-3 and I-7 (namely P3 and P7, respectively) served as peptide backbone and we designed a novel folate targeting peptide-PTX conjugates to achieve selective tumor delivery, enhance cellular uptake, make FA-P3/P7-PTX conjugates water-soluble and overcome drug resistance. The conjugates were evaluated for the antiproliferative activity in different cancer cell lines, the inhibitory rate of tubulin polymerization, hemolytic toxicity and water solubility (more than 20 mg/mL, Fig. S5). Furthermore, we assessed the conjugates for their cellular uptake, Membrane permeability, pro-apoptosis, alternation of mitochondrial membrane potential, rat plasma stability and cell apoptosis pathway in PTX resistant MCF-7/PTX cells. Finally, we researched the most optimized conjugate in vivo antitumor efficacy compared with free PTX.

2. Results and discussion

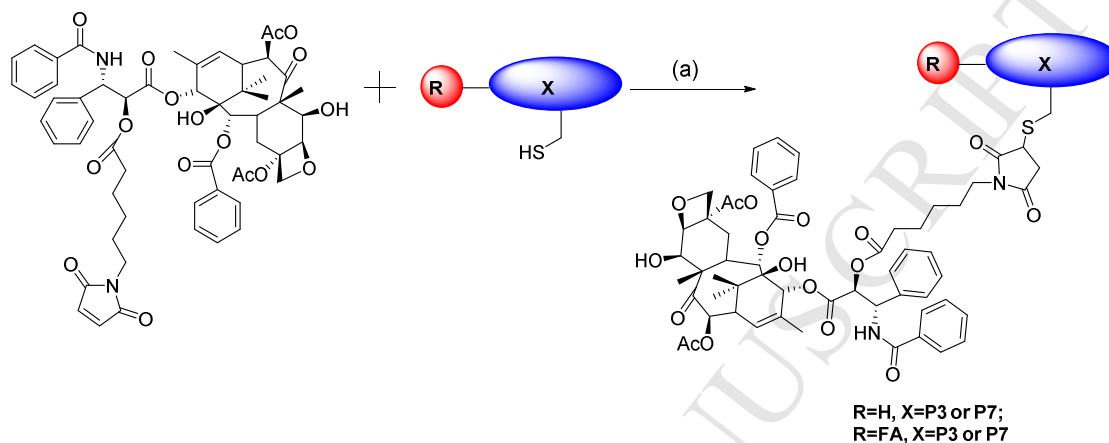
2.1 Synthesis of FA-targeting conjugates



Scheme 1. Synthesis Route of Paclitaxel maleimide. ^aReagents and conditions: (a) glacial acetic acid, reflux; (b)SOCl₂, DCM, N₂; (c)TEA, DCM, N₂



Scheme 2. Synthesis route of N¹⁰-TFA-Pteric Acid. (a). (i) TFAA, (ii) 3% TFA.

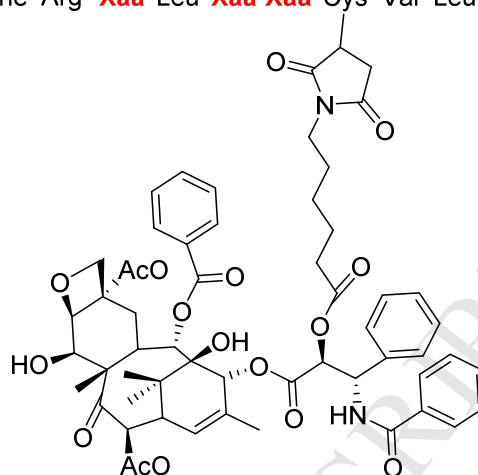


Scheme 3. Solid phase synthesis of conjugates. (a) Sodium phosphate buffer (pH 7.0), 25°C.

Novel peptide-drug conjugates based on PTX coupled with lytic membrane peptide and folic acid modifiers were designed and synthesized (Table 1 and Fig.S1). The objective was to combine a set of desirable physicochemical, biochemical, and chemotherapeutic properties into a single integrated macromolecule structure. As shown in Scheme 1, PTX was modified by maleimide, since maleimide undergoes Michael additions with thiol groups at neutral pH. Cysteine containing peptides were synthesized by using a solid phase methodology according to the previously reported procedure³⁹. As shown in Scheme 2 and Scheme 3, the thiol group in cysteine moiety was used to conjugate with PTX-maleimide and N-terminal of peptide was used for conjugation of folic acid. The purities of the four conjugates were all above 95%. The observed multiply charged ions of the conjugates were shown in Table 2 and Fig.S6, by ESI mass spectrometry.

Table 1 Structures of the conjugates

5
10
15
R-Leu-Val-**Xaa**-Arg-Phe-**Xaa**-**Xaa**-Phe-Phe-Arg-**Xaa**-Leu-**Xaa**-**Xaa**-Cys-Val-Leu-Leu-NH₂



Compounds	R	Xaa
P3-PTX	H	
FA-P3-PTX		
P7-PTX	H	
FA-P7-PTX		

Table 2. Characterization of the conjugates^a

Compounds	Molecular formula	Molecular weight	Mass (Da)			
			Calculated	Observed		
FA-P3-PTX	C ₁₈₈ H ₂₇₂ N ₄₀ O ₄₀ S	3764.54	[M+4H] ⁴⁺	942.1	[M+4H] ⁴⁺	942.5

			[M+5H] ⁵⁺	753.9	[M+5H] ⁵⁺	754.7
P3-PTX	C ₁₆₉ H ₂₅₄ N ₃₃ O ₃₅ S	3341.15	[M+4H] ⁴⁺	836.0	[M+4H] ⁴⁺	837.2
			[M+5H] ⁵⁺	669.0	[M+5H] ⁵⁺	669.9
FA-P7-PTX	C ₁₈₈ H ₂₇₂ N ₅₂ O ₄₀ S	3933.63	[M+4H] ⁴⁺	984.2	[M+4H] ⁴⁺	984.9
			[M+5H] ⁵⁺	787.5	[M+5H] ⁵⁺	788.3
P7-PTX	C ₁₆₉ H ₂₅₄ N ₄₅ O ₃ S	3509.23	[M+4H] ⁴⁺	878.1	[M+4H] ⁴⁺	878.9
			[M+5H] ⁵⁺	702.7	[M+5H] ⁵⁺	703.2

^aUPLC conditions: 10–80% acetonitrile (mobile phase A: water with 0.1% formic acid, mobile phase B: acetonitrile with 0.1% formic acid) in 10 min at a flow rate of 0.3 mL/min with ultraviolet (UV) detection at 214 nm with the use of Waters ACQUITY UPLCBEH C18 column (1.7 × 50 mm, Waters)

2.2 Cytotoxicity and Hemolytic Activity

Table 3 Anti-tumor activity of the conjugates

Compounds	IC ₅₀ (μM)					
	MCF-7	MCF-7/PTX	K562	A2780	SKOV3	HUVEC
FA-P3-PTX	1.79±0.09 [#]	4.54±0.71 ^{*,#}	5.38±0.25	1.95±0.20 ^{*,#}	5.92±0.84	48.55±2.94 ^{*,##}
P3-PTX	2.15±0.18	6.11±0.61 ^{**}	5.90±0.92	2.69±0.19	7.17±0.77	31.60±1.88 ^{**}
FA-P7-PTX	1.39±0.12 [#]	2.92±0.2 ^{*,##}	3.85±0.9 [*]	1.42±0.08 ^{*,##}	5.49±0.36	45.21±1.79 ^{*,##}
P7-PTX	1.98±0.14	5.53±0.76 ^{**}	3.82±0.29 ^{**}	2.79±0.17	6.61±0.94	37.22±2.36 ^{**}
P3	12.31±0.96 ^{**}	15.24±1.53 ^{**}	13.65±1.30 ^{**}	13.56±1.72 ^{**}	14.69±1.10 ^{**}	40.17±1.92 ^{**}
P7	8.61±0.86 ^{**}	17.08±1.32 ^{**}	9.49±0.80 ^{**}	11.50±1.37 ^{**}	13.58±1.28 ^{**}	44.53±2.61 ^{**}
PTX	1.17±0.29	54.8±2.83	5.80±0.40	2.85±0.40	6.29 ± 0.73	9.39±0.98

^a Notes: PTX: paclitaxel. *P < 0.05. **P < 0.01 vs PTX; #P < 0.05. ##P < 0.01 (FA-P3-PTX vs P3-PTX or FA-P7-PTX vs P7-PTX).

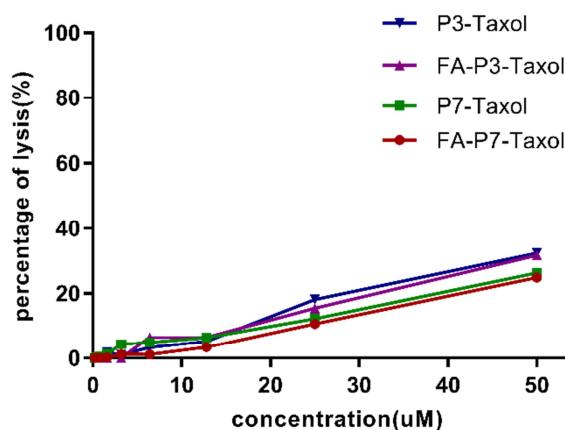


Fig. 1 Hemolysis effects on RBCs of the conjugates. Various concentrations of P3-PTX, FA-P3-PTX, P7-PTX and FA-P7-PTX were incubated with RBCs. The results shown all the tested peptides exhibited modest hemolytic activity

The anticancer activities of the conjugates were evaluated using various cancer cells (MCF-7, MCF-7/PTX, K562, A2780 and SKOV3). The IC_{50} values are listed in Table 3, and PTX was used for comparison. All the conjugates exhibited improved cytotoxic effects on various cancer cells. According to the results, all the conjugates showed significantly stronger antiproliferative activity than former lytic peptides (P3 and P7), and FA-P3-PTX and FA-P7-PTX showed more excellent antiproliferative activity than P3-PTX and P7-PTX in FA-overexpressing cancer cells MCF-7 (1.79 uM versus 2.15 uM; 1.39 uM versus 1.98 uM), MCF-7/PTX (4.54 uM versus 6.11 uM; 2.92 uM versus 5.53 uM), A2780 (1.95 uM versus 2.69 uM; 1.42 uM versus 2.79 uM), respectively. Thus, the conjugate FA-P3-PTX and FA-P7-PTX exhibited great antiproliferative activity on folate receptors overexpressing cancer cells, and almost equal potency to both drug resistant and -sensitive cells. Meanwhile, the conjugates showed weak toxicity to the normal cell lines HUVEC. To assess the safety profile of the designed conjugates, we examined their hemolytic activity using RBCs. As depicted in Fig. 1, all the tested peptides exhibited modest hemolytic activity.

2.3 Concentration Dependent Cellular Uptake

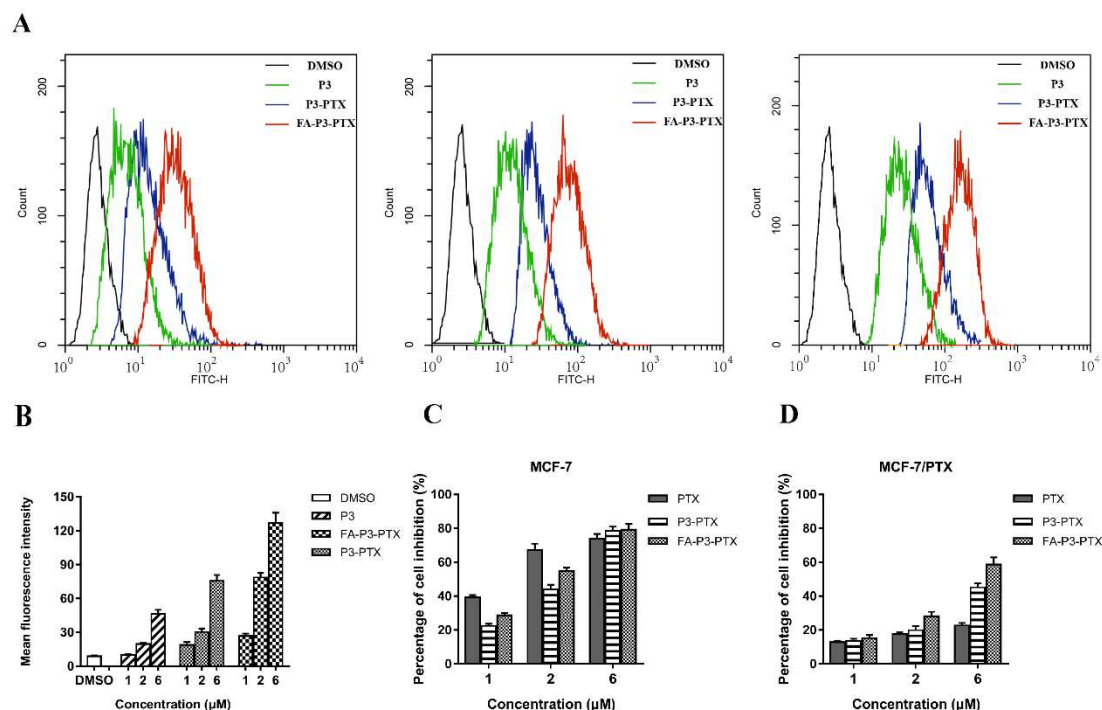


Fig. 2 Concentration-dependent cellular uptake of P3_{FITC}, P3-PTX_{FITC} and FA-P3-PTX_{FITC} by drug resistant MCF-7/PTX cells. (A) Representative flow cytometry spectra of the cells treated with 1, 2, or 6 μM different drugs for 2 h, and untreated cells as control; (B) quantitative comparison of the fluorescence intensity in the studied from endocytosed drugs after 2 h treatment with 1, 2, or 6 μM drugs.; (C) and (D) Cell viability of drug sensitive MCF-7 cells (C) and resistant MCF-7/PTX cells (D) after treatment with PTX, P3-PTX, or FA-P3-PTX at three different concentrations (1, 2, and 6 μM).

To obtain quantitative information on the concentration-dependent cellular uptake, FITC labeled conjugates were synthesized (Table S1). We used flow cytometry to track endocytosed conjugates in drug resistant breast MCF-7/PTX cancer cells.

The respective low fluorescent intensities suggested low accumulated concentration of the dye or drug within cells. Simultaneously, the increase in fluorescence intensity for labelled conjugates implied that an active cellular uptake mechanism may be involved. In cases of the conjugates, it was evident that the endocytosis of FA-P3-PTX_{FITC} was higher than P3-PTX_{FITC} at the same concentration, visibly suggested that the conjugation FA has a significant influence on the cellular uptake (Fig. 2A and 2B). Next, we performed cytotoxicity experiments of the conjugates against MCF-7 and MCF-7/PTX cells, to study the relationship of cellular uptake and cytotoxicity. For the drug resistant MCF-7/PTX cells, the cytotoxicity of free PTX dropped dramatically, with no significant cytotoxicity observed (Fig. 2C and 2D). In contrast, conjugate FA-P3-PTX showed consistent cytotoxicity against both the sensitive and resistant cell lines. This result indicated that acquired drug resistant not greatly affected the antitumor activities of the drug conjugates, as is the case for free PTX.

2.4 Membrane Permeability

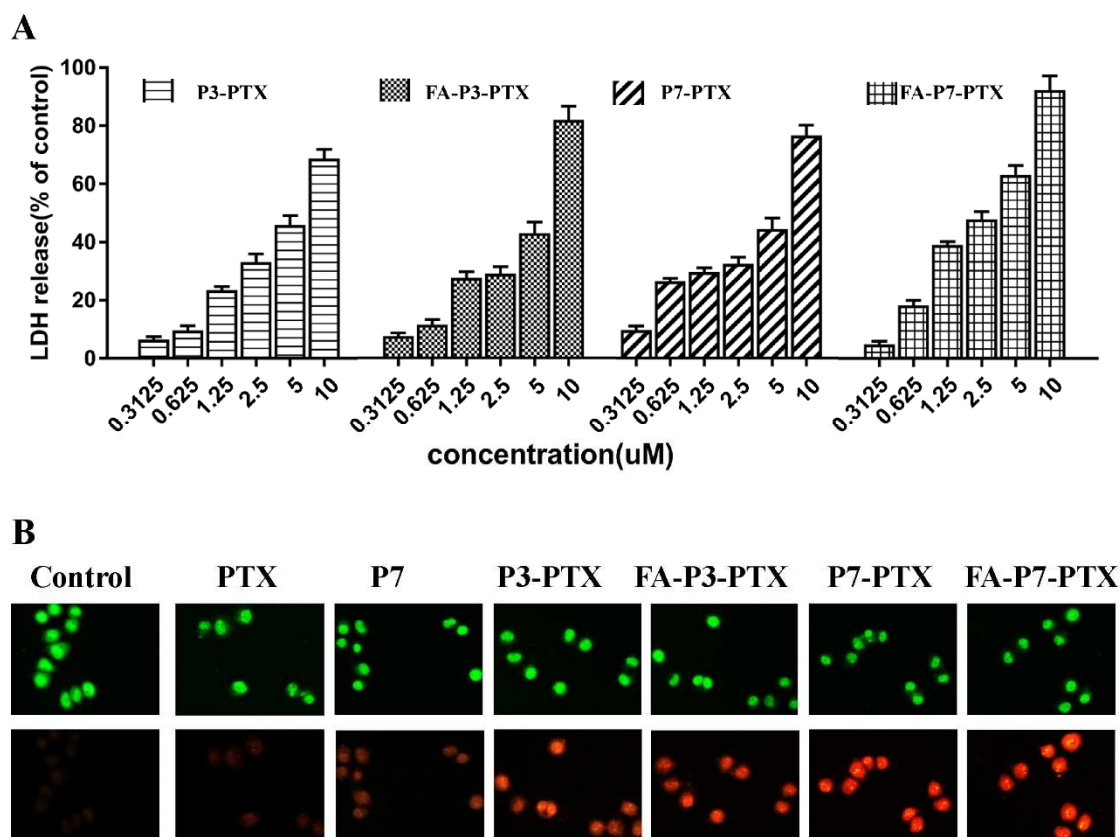


Fig. 3 (A) LDH leakage assay of drug conjugates; (B) AO/EB staining images in MCF-7/PTX cells after treatment with 3 μ M of PTX, P7, P3-PTX, FA-P3-PTX, P7-PTX and FA-P7-PTX, respectively. 0.1% DMSO served as control.

To research if the conjugates reserved property with the disruptive membrane of lytic peptides, we designed lactate dehydrogenase (LDH) leakage assay as previous reported⁴⁰⁻⁴¹. Membrane lysis activity of the conjugates confirmed by measuring release of the ubiquitous, cytoplasmic enzyme LDH in the culture medium. MCF-7/PTX cells were incubated with different concentrations of drug conjugates (FA-P3-PTX, P3-PTX, FA-P7-PTX and P7-PTX,) and the results exhibited that the drug conjugates caused the release of the cytosolic LDH enzyme in a concentration-dependent manner (Fig. 3A). Notably, as shown in Table 3 and Fig. 3A, FA-P3-PTX and FA-P7-PTX possessed more excellent anti-cancer activity in

MCF-7/PTX cells and stronger disruptive membrane activity. To further validated, visualization of AO/EB double staining test were utilized to detect membrane integrity in MCF-7/PTX cells. AO can stain both live and dead cells and presents green fluorescence. EB stains only apoptotic or necrotic cells that have lost their membrane integrity and shows red fluorescence. As shown in Fig. 3B, MCF-7/PTX cells displayed red fluorescence all after treatment with the drug conjugates (3 μ M of drug conjugates) for 12 h.

Thus, these results demonstrated that the drug conjugates with the character of lytic peptides could seriously disrupt the membrane and alter the penetrability to strengthen the cytotoxicity activity of conjugates. FA-P3-PTX and FA-P7-PTX drug conjugates were selected for further investigation. In addition, the clearly morphological features of AO/EB double staining preliminary indicated that the drug conjugates can induce apoptosis of MCF-7/PTX cells.

2.5 Pro-apoptotic Assay

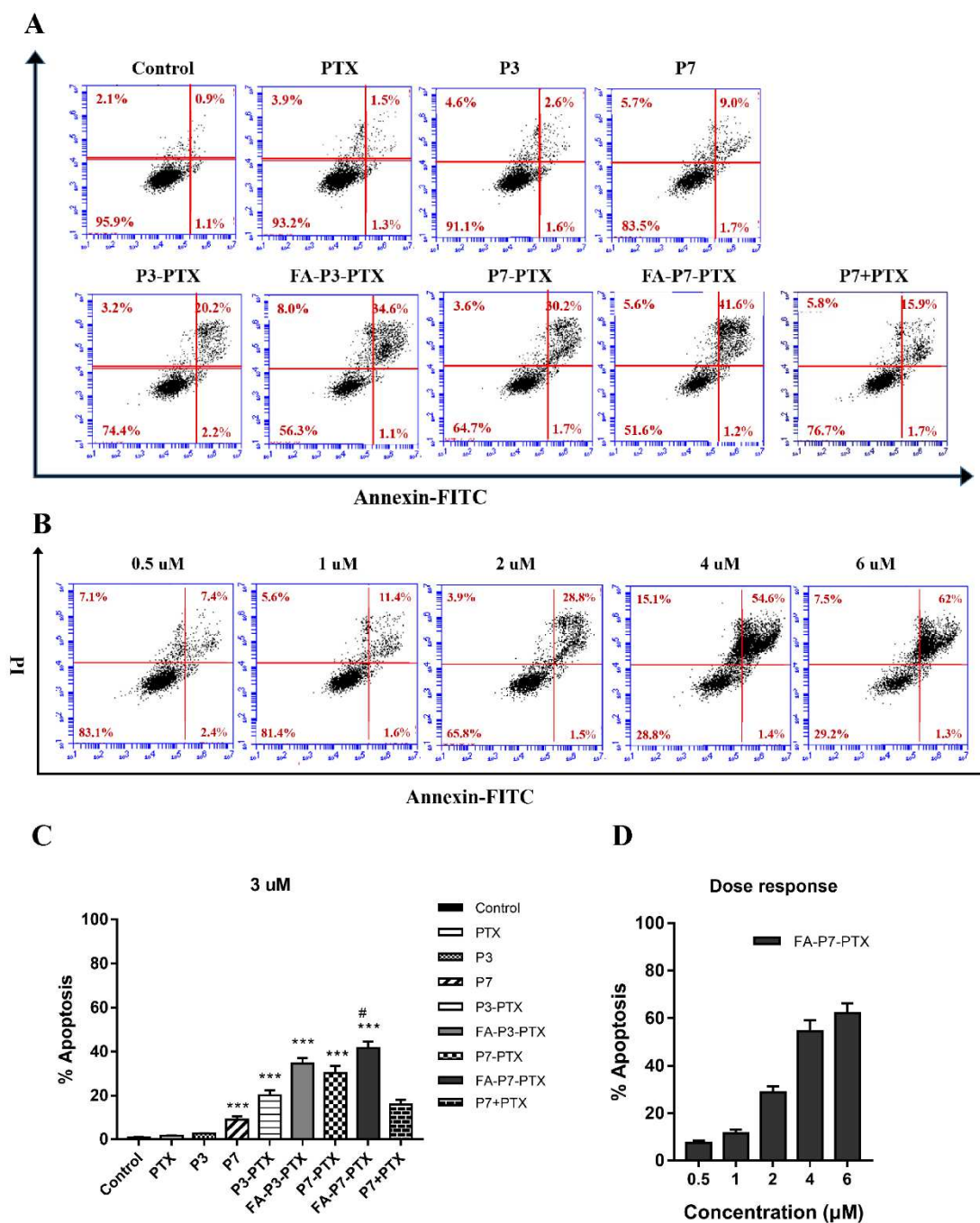


Fig. 4 The conjugates induced apoptosis in MCF-7/PTX cells. (A) Cells were treated with 3 uM of conjugates for 12 h. Control samples were treated with 0.1% DMSO; (B) Cells were treated with 0.5, 1, 2, 4, and 6 uM of FA-P7-PTX. Percentage of apoptosis was measured by flow cytometry;

(C) Quantitative data from the apoptosis measurement described in (A), *P < 0.05. **P < 0.01. ***P < 0.001 vs control, #P < 0.05 (FA-P7-PTX vs FA-P3-PTX).; (D) Quantitative data from the apoptosis measurement described in (B).

To further confirm the nature of drug resistance cell death induced by compounds, the effect on drug resistant MCF-7/PTX cells apoptosis analysis was determined indirectly using Flow Cytometer with Annexin-FITC/PI staining. Preliminary flow cytometric analysis MCF-7/PTX cell lines treated under identical conditions with all the drug conjugates (3 μ M) evidenced that FA drug conjugates were able to induce the more pro-apoptotic, while 3 μ M of FA-P3-PTX and FA-P7-PTX induced 34.6 and 41.6 % MCF-7/PTX cell apoptosis respectively (Fig. 4A and 4C).

Thus, FA-P7-PTX possessed stronger pro-apoptotic activity compared to FA-P3-PTX. As shown in Fig. 4B and 4D, apoptosis ratio appeared concentration-dependent increase after MCF-7/PTX cells were treated with FA-P7-PTX with concentration of 0.5 μ M to 6 μ M.

2.6 Cellular Colocalization

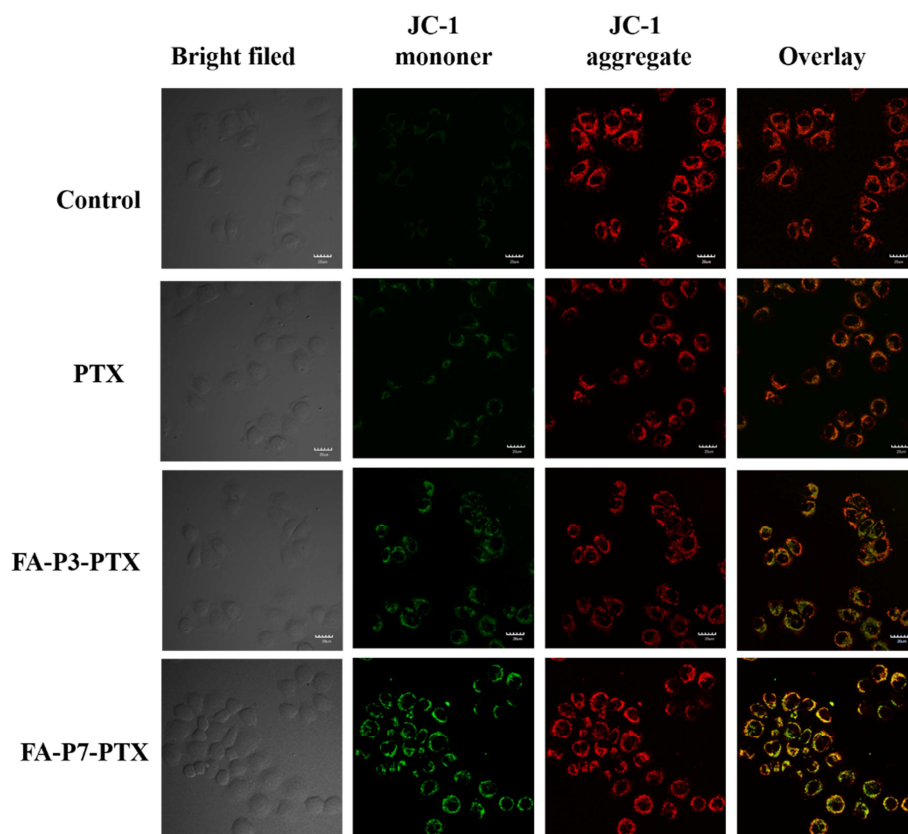


Fig. 5. Conjugates induced mitochondrial dysfunction. Fluorescence microscope analysis of cellular mitochondrial transmembrane potential level by JC-1 staining after 3 μ M of PTX, FA-P3-PTX and FA-P7-PTX treatment for 12 h. 0.1% DMSO was served as control.

Mitochondria are the essential parameter of the two main apoptotic signaling pathway, namely the intrinsic and extrinsic pathways⁴²⁻⁴³. To recognize if FA-P3-PTX and FA-P7-PTX induce apoptosis by targeting mitochondria, we measured the loss of mitochondrial transmembrane potential by a fluorescence dye JC-1, a mitochondrial membrane-potential-sensitive dye, which act as reliable indicator of the dissipation of mitochondrial membrane, observed as red fluorescence to green⁴⁴. As shown in Fig. 5, a significant alteration of fluorescence owing to loss of mitochondrial membrane potential was observed following MCF-7/PTX cells treatment with FA-P3-PTX and FA-P7-PTX compared with control (Fig. 7B) indicating that these novel drug conjugates induced apoptosis by targeting the mitochondria.

Collectively, the results provide evidence that drug conjugates FA-P3-PTX and FA-P7-PTX are able to induce cell death by apoptosis through a mitochondrial dependent pathway with FA-P7-PTX being the most active of the series.

2.7 Western Blot Analysis of Caspase-3, Cytochrome-C and Folate receptor.

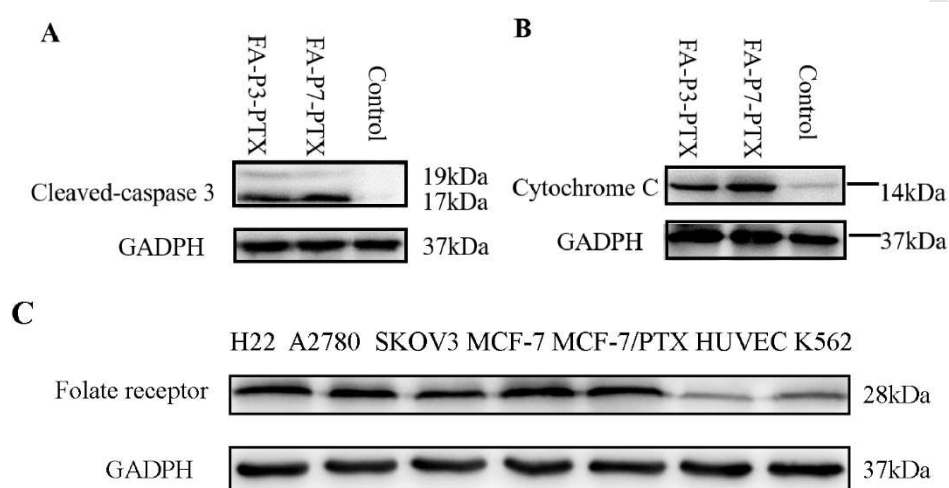
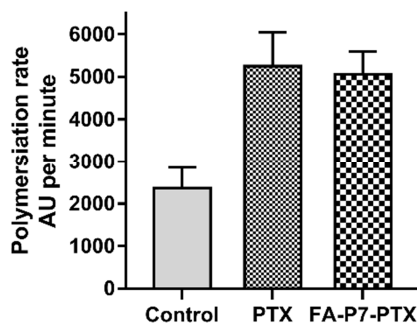


Fig. 6 (A) The western blot analysis of cleaved-caspase-3 for MCF-7/PTX cells; (B) The western blot analysis of Cytochrome C. (C) The western blot analysis of folate receptor on the cell lines. GADPH was probed as loading control.

The disrupted mitochondrial can release pro-apoptotic factors such as cytochrome c and other apoptosis inducing factors⁴⁵. Caspases also are the important parameter of initiation and performance of apoptosis and the apoptotic signaling pathway consist of the extrinsic and intrinsic pathways, which are dependent on the cleavage of caspases⁴⁶. The activation of Caspase-3 is a crucial regulatory protein of cell apoptosis. To further explain the mechanism of drug resistance cells apoptosis induced by FA-P3-PTX and FA-P7-PTX, the activities of cleaved caspase-3 and cytochrome C were examined. As shown in Fig. 6A and 6B, MCF-7/PTX cells treatment with 3 μ M of FA-P3-PTX and FA-P7-PTX for 2 h, exhibits dramatic enhancement in cleaved caspase-3 and Cytochrome-C in the cytoplasm. As shown in Fig. 6C, the results shown that MCF-7, MCF-7/PTX and A2780 had higher

expression quantities of folate receptor than that of other cells.

This result further confirms that FA-P3-PTX and FA-P7-PTX induces mitochondrial dysfunction and caspase-3-dependent apoptotic cell death in MCF-7/PTX cells.



2.8 Tubulin Polymerization Assay

Fig 7. In vitro tubulin polymerization induced by 3 μ M of PTX and FA-P7-PTX.

The results shown that at equimolar concentrations, polymerization induced by FA-P7-PTX was slightly lower than PTX. This may not affect the antitumor activity of FA-P7-PTX.

2.9 Stability of the FA-P7-PTX in Rat Plasma

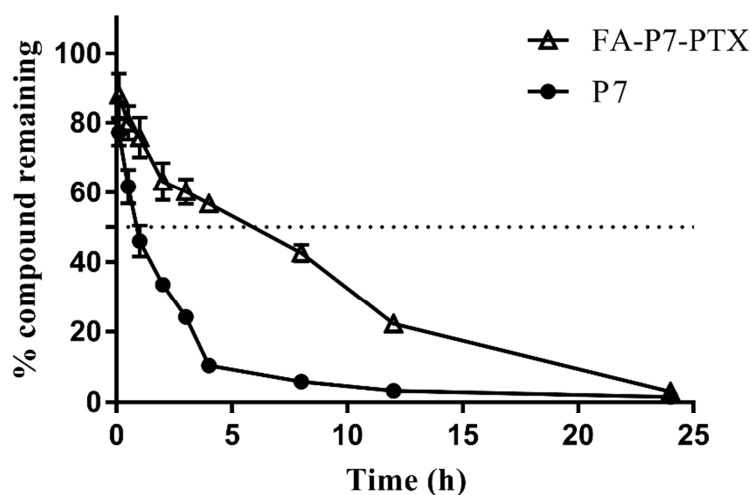


Fig.8 Time-dependent stability of P7 and FA-P7-PTX in rat plasma monitored over 24 h.

FA-P7-PTX were incubated with plasma over 24 h and compared with P7. Aliquots were removed at different time points (0.1,0.5, 1, 2, 3, 4, 8, 12, 24, h) for analysis using UPLC/MS. Fig. 8 displayed the time profile of conjugates degradation. As expected, FA-P7-PTX was more stable to proteolytic degradation compared to P7. FA-P7-PTX possessed a half-life of ~5.9 h at 37 °C, while P7 the half-life was 0.8 h. These data revealed that FA-P7-PTX is stable enough to allow sufficient time for cancer cell targeting.

2.10 *In Vivo* Antitumor Efficacy

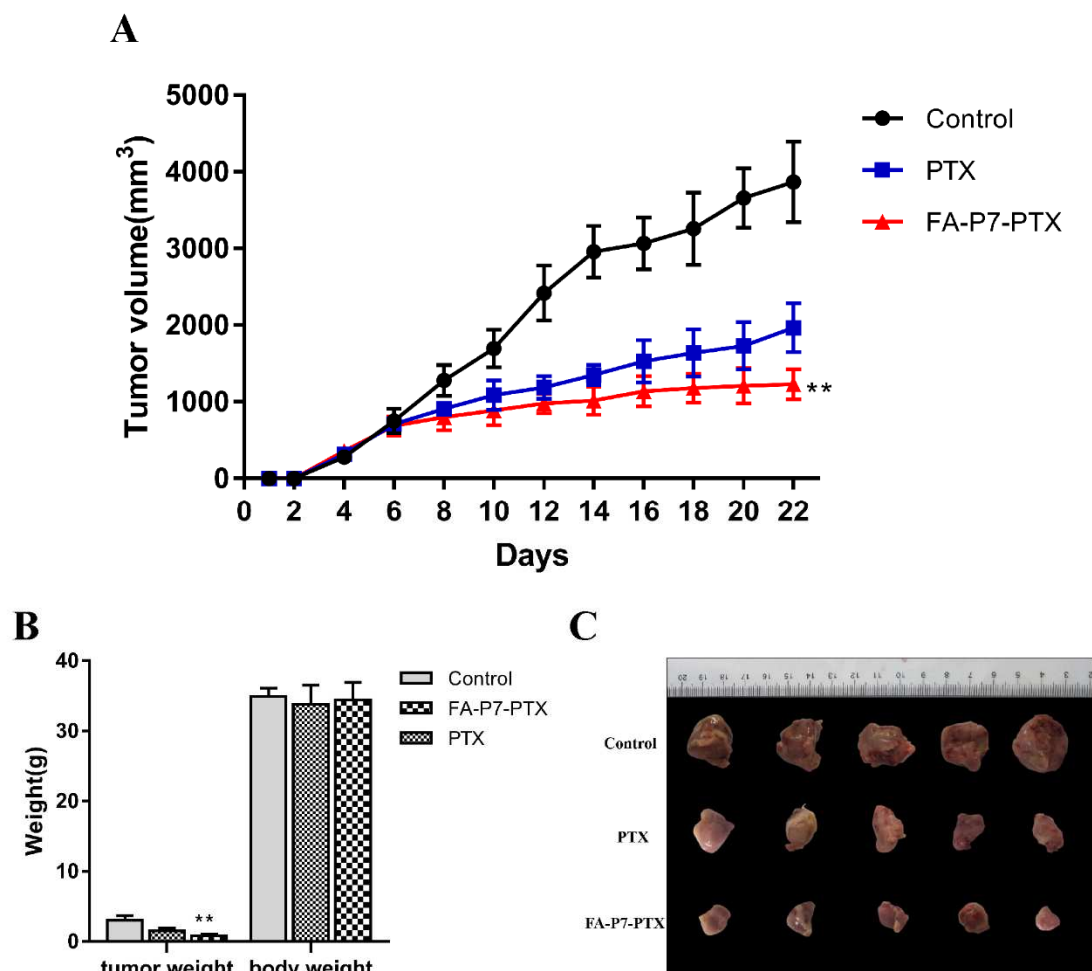


Fig. 9 (A) Tumor volume curve of H22 mice model over time when treated with FA-P7-PTX (12 $\mu\text{mol/kg}$), PTX (12 $\mu\text{mol/kg}$) or 0.9% saline. Tumor volumes were measured by calipers; (B) Tumor weight and body weight. * $P < 0.05$. ** $P < 0.01$ vs PTX, Values represent the means \pm SD. (C) Photos of tumors separated from mice.

To study the anticancer activity of FA-P7-PTX *in vivo*, we performed tumor-bearing mice model with H22 cells by administering once every two days peritumoral injection of FA-P7-PTX (12 $\mu\text{mol/kg}$), PTX (12 $\mu\text{mol/kg}$, as the positive control), or 0.9% saline as the negative control for 2 weeks. Compared with control group, the tumor volumes of the FA-P7-PTX group were dramatically reduced by 69% with no significant variation in mouse body weight (Fig. 9). Meanwhile, FA-P7-PTX exhibited stronger inhibitory effects on tumor volume compared with PTX (69% versus 49%). The result confirmed that FA-P7-PTX possessed higher potency in slowing the growth of solid tumors.

3. Conclusion

In conclusion, we have successfully developed novel folate receptors targeted drug conjugates by incorporating lytic peptides, which serves as a linker of the FA and PTX (Table 1). FA-P3-PTX and FA-P7-PTX showed significantly higher antiproliferative activity than PTX in MCF-7/PTX and A2780 cells when compared with PTX which showed comparable activity against MCF-7, K562 and SKOV3 cells (Table 3). FA-P3-PTX_{FITC} exhibited higher cellular uptake in MCF-7/PTX cells as shown by flow cytometry when compared with P3-PTX_{FITC}, which demonstrated that the increased cellular uptake dependent on FR (Fig. 2). FA-P3-PTX and FA-P7-PTX presented stronger membrane disrupting activity in MCF-7/PTX cells with a concentration-dependent manner. The AO/EB double staining test also ascertained evidence of the disruption to MCF-7/PTX cell membranes (Fig. 3). Meanwhile, FA-P3-PTX and FA-P7-PTX exhibited little hemolysis activity against the RBCs (Fig. 1). The Annexin-FITC/PI staining proved that the pro-apoptosis proportion of FA-P7-PTX was much greater than the control and better than that of FA-P3-PTX with a dose-dependent manner (Fig. 4). Compared to FA-P3-PTX, FA-P7-PTX revealed much stronger effects on cell toxicity, membrane disrupting activity and pro-apoptosis in MCF-7/PTX cells. The anti-cancer mechanisms of FA-P3-PTX and FA-P7-PTX might be a mitochondrial impairment and caspase-3-dependent apoptotic cell death (Fig. 5 and Fig. 6). Meanwhile, the rat plasma stability revealed that FA-P7-PTX exhibited favorable plasma stability over P7 (Fig. 8). Furthermore, the in vivo antitumor efficacy study confirmed that FA-P7-PTX performed more stronger potency in inhibition of tumors growth than PTX (Fig. 9).

In summary, the present work signifies that the conjugate FA-P7-PTX may be a promising candidate for drug-resistant cancer therapy.

4. Experimental section

4.1 Materials and Animals

All reagents were purchased as reagent grade and used without further purification. N^α-Protected amino acids, Fmoc-Arg(Pdf)-OH, Fmoc-Leu-OH, Fmoc-Val-OH and Rink amide MBHA resin (loading 0.557 mmol g⁻¹), were purchased from GL Biochem Ltd. (Shanghai, China). Fmoc-Glu-OtBu, Fmoc-Lys (Boc)-OH, Fmoc-Phe-OH, Fmoc-Cys(Trt)-OH and N-Hydroxybenzotriazole (HOBt), were purchased from Nanjing Peptide Biotech Ltd. N, N-diisopropylcarbodiimide (DIC), trifluoroacetic acid (TFA), N, N-diisopropylethyl amine (DIPEA) and Trifluoroacetic anhydride(TFAA) were purchased from Energy chemical. Paclitaxel was purchased from Ark Pharm. Pteric acid was purchased from Bide Pharmatech. Fluorescein isothiocyanate isomer (FITC) was purchased from Aladdin. All other reagents, unless otherwise indicated, were obtained from Sigma-Aldrich Co. (Saint Louis, MO) and used as received. LDH Activity Assay Kit was purchased from Nanjing Jiancheng Bioengineering Institute. RIPA buffer, Membrane Potential Assay Kit and BCA Protein Assay Kit were purchased from Beyotime Biotechnology. Annexin V-FITC/PI Detection Kit and Cell Cycle Detection Kit were purchased from KeyGEN BioTECH. Rabbit polyclonal antibody (CASP3 polyclonal antibody, GAPDH polyclonal antibody, Cytochrome C) were purchased from ABclonal. Microwave procedures were performed in the Microwave Peptide Synthesizer (CEM, Matthews, NC, USA).

4.2 Synthesis of the peptides

The peptides were synthesized by the standard solid-phase peptide synthesis protocol of standard Fmoc strategy on Rink amide MBHA resin, as already described in previous research⁴⁷. HBTU/HOBt/DIPEA was used for the coupling procedure of amine acid and piperidine/DMF (20%, v/v) was used for deprotection of N-terminal

Fmoc group. For peptides P3 and FA-P3, the Dde protection of Lys3 was removed by hydrazine/DMF (2% , v/v) for 3 times for 10 min at 25°. The result was detected by Kaiser test. Then Fmoc-β-Ala-OH was coupled by DIC/HOBt. Fmoc group was removed and FITC labeling was performed with the solution of FITC (4 equiv) and DIPEA (12 equiv) in DMF in the dark overnight. Completed Rink amide MBHA resins were treated with Reagent K (TFA/EDT/water/phenol/thioanisole, 82.5:2.5:5:5:5) for 4 h. Cold Et₂O was used to separate out the crude peptide, which was purified by preparative RP-HPLC. The reaction mixture was filtered and washed by DCM two times.

4.3 Synthesis of the PTX maleimide (5)

General procedure for preparation of compound 3 has been reported in previous research³⁹. Then, compound 3 (422 mg, 2 mmol) was dissolved in 20 ml of anhydrous DCM which was then reacted with 10 equiv of SOCl₂ at 0 °C for 1 h to produce the desired intermediate compound 4. PTX (854mg, 1mmol) and 350ul of trimethylamine (TEA) were dissolved in 10ml of anhydrous DCM, and then compound 4 was added at 0° under Ar atmosphere. The resulting solution was stirred for 2 h at the dark. The reaction mixture with Ar atmosphere protection was evaporated under vacuum. Compound 5 was obtained by column chromatography (DCM: Methanol, 20:1) with a yield of 58% (Scheme 1). ¹H NMR (300 MHz, DMSO-d₆) δ 9.29-9.26 (d, *J*=9.24 Hz, 1H), 8.00-7.96 (t, *J*=12.56 Hz, 3H), 7.88-7.86 (d, *J*=6.12 Hz, 2H), 7.77-7.64 (m, 3H), 7.58-7.45 (m, 7H), 7.18-7.20 (t, *J*=6.07 Hz, 1H), 6.99 (s, 2H), 6.30 (s, 1H), 5.84-5.78 (t, *J*=18.04 Hz, 1H), 5.57-5.51 (t, *J*=18.16 Hz, 1H), 5.43-5.33 (m, 2H), 4.93-4.90 (m, 2H), 4.64 (s, 1H), 4.12-4.02 (m, 3H), 3.60-3.58 (d, *J*=6.78 Hz, 1H), 3.28 (m, 1H), 2.89 (s, 2H), 2.73 (s, 2H), 2.31 (s, 3H), 2.25 (s, 3H), 1.77-1.71 (m, 3H), 1.60-1.40 (m, 6H), 1.30-1.19 (m, 5H), 1.03-1.01 (d, *J*=6.46 Hz, 6H). MS (ESI) *m/z* calcd for [C₅₇H₆₂N₂O₁₇ + Na]⁺ calcd. for 1070.12; found, 1070.5.

4.4 Synthesis of N^{10} -TFA-Pterioic Acid

Pterioic acid (624 mg, 2 mmol) was dissolved in 4ml of trifluoroacetic anhydride (TFFA) and stirred under nitrogen in the dark for 2 h. The mixture was concentrated under reduced pressure by rotary evaporator. Then, 20 ml of 3% TFA was added, and the resulting solution was neutralized with $\text{NH}_4\text{OH}(\text{aq})$. 590 mg of pale yellow solid (compound 7) was obtained (yield 72%, Scheme 2). ^1H NMR (400 MHz, DMSO-d_6) δ 4.48 (m, 2H); 6.66-6.65 (d, $J = 4.27$ Hz, 2H); 7.68-7.65 (d, $J = 12.04$ Hz, 2H); 8.67-8.64 (m, 2H); 11.53 (s, 1H); MS (ESI) m/z calcd for $[\text{C}_{16}\text{H}_{12}\text{F}_3\text{N}_6\text{O}_4 + \text{H}]^+$ calcd. for 409.29; found, 409.6.

4.5 Synthesis and purification of the conjugates

The peptides (P3: LVKRFKKFFRKLKKCVLL- NH_2 , P7: LVRRFRRFFRRLRRCVLL- NH_2) with cysteine were synthesized on Rink-amide-MBHA (4-methyl-benzylhydramine) resin using Fmoc-based solid phase peptide synthesis (SPPS) as previously reported⁴⁷.

0.1 mmol of the cysteine-containing peptides (P3, P7, FA-P3, FA-P7, $\text{FITC-}\beta\text{A}P3$ and $\text{FITC-}\beta\text{A}FA-P3$) were dissolved in 5 mL of 0.05 $\text{mol}\cdot\text{L}^{-1}$ sodium phosphate buffer (pH 7.0), then, added methanol solution of compound 5 (107 mg, 0.1 mmol) slowly. The reaction mixture was stirred at 25 $^\circ\text{C}$ for 12 h until the reaction was complete (Scheme 3). Purification of crude conjugate was carried out by RP-HPLC on a C18 column (Shimadzu LC-10). RP-HPLC conditions: 10–80% acetonitrile (mobile phase A: water with 0.1% TFA, mobile phase B: acetonitrile with 0.1% TFA) in 60 min at a flow rate of 10 mL/min with ultraviolet (UV) detection at 214 nm. All the conjugates purities were monitored by UPLC/MS (Waters UPLC with the ACQUITY TQD; Waters Corporation, Milford, MA, USA) with a Waters ACQUITY UPLCBEH C18 column (1.7 \times 50 mm, Waters). The purities of the conjugates were above 95%.

4.6 Cell Culture

Human ovarian cancer cell lines A2780 and SKOV3, leukemia cells K562, human breast cancer cell lines MCF-7, paclitaxel resistant sub-line MCF-7/PTX, human gastric mucosal epithelial cells GES-1 and mouse H22 hepatoma cells, were obtained from KeyGEN BioTECH (Nanjing, China). K562, MCF-7, MCF-7/PTX, H22 and GES-1 cells were cultured in RPMI 1640 supplied with 10% fetal calf serum (FBS, Hyclone Laboratories). A2780 cells were grown in DMEM supplemented with 10% FBS. SKOV3 cells were cultured in McCoy's 5A supplemented with 10% FBS. All media were supplemented with 1% penicillin/streptomycin antibiotics (GibcoBRL). All the cells were incubated at 37 °C in a humidified 5% CO₂.

4.7 Cytotoxicity Assay

Cell viability was evaluated by MTT method with a minor modification³⁸. cells during logarithmic growth phase were seeded in 96-well plates at 6×10^3 cells per well and incubated overnight. The conjugates were added to cells with various final concentrations (ranging from 0.4 μ M to 50 μ M) and incubated in a 37 °C incubator containing 5% CO₂ for 48 h. MTT dye (10 μ L of 5 mg/mL in PBS) was added to each well 4 h. The plates were then centrifuged at 1500 rpm for 10 min and the supernatant was removed without distracting the formazan precipitate and cells in the wells. Next, 150 μ L of DMSO was added to dissolve formazan crystals and the plates agitated on a plate shaker for 5 min. The absorbance at 490 nm was detected in a microplate reader (Thermo, USA). The IC₅₀ values of conjugates were calculated by GraphPad Prism 7.0 software (San Diego, CA, USA) on the basis of the dose–response curves. Assays were examined three times.

4.8 Hemolysis Activity

Wistar rats (male, 18–22 g, Certificate number: NO.201824693) were purchased

from the Comparative Medical Center of Yangzhou University (Jiangsu, China). All the animals involved were treated in accordance with protocols approved by the ethical committee of China Pharmaceutical University. All animal experimental protocols adhered to the Guide for the Care and Use of Laboratory Animals published by the National Institutes of Health (NIH publication 85-23, revised 1986). Hemolytic activity was determined by a standard procedure against mouse erythrocytes. Briefly, the erythrocytes were diluted to 5×10^8 /mL, and 250 μ L of erythrocytes solution were incubated for 1 h with various concentrations of conjugates at 37 °C. Intact erythrocytes were centrifuged at 1500 rpm for 10 min, and the absorbance of the supernatant at 540 nm was measured by a microplate reader (Thermo, USA). 1% Triton X-100 was set as a positive control, and PBS buffer served as a negative control.

4.9 Cellular uptake of conjugates

To investigate if the cell penetration efficiency of the conjugates would be affected by folate receptor, the cellular uptake of the FITCFA-P3-PTX, FITCP3-PTX, and FITCP3 were compared. Adherent MCF-7/PTX cells were seeded overnight in 12-well plates and then treated with labelled conjugates at various concentrations (1, 2, and 6 μ M) for different periods of time for 2 h. Then cells were collected and washed with cold PBS for three times. The cellular fluorescence intensities of about 10000 cells treated by respective compounds were analyzed each time using a flow cytometer.

4.10 LDH leakage assay

The LDH leakage assay was used to determine the membrane integrity by using a commercial LDH Activity Assay Kit (Nanjing Jiancheng Bioengineering Institute)⁴⁸. The LDH assay was accomplished according to the manufacturer's protocols. Briefly, MCF-7/PTX cells were seeded in a 96-well plate (6×10^3 cells per well) and

incubated for 24 h. Next, the serum-free medium containing the various concentrations of conjugates was added and incubated for 12 h. The plates were centrifuged ($3000 \times g$, 10 min) and supernatants were transferred to a new 96-well plate. PBS buffer was added as a negative control which was taken as no leakage. The absorbance was detected by microplate reader at 450 nm. The cells treated with 1% Triton X-100 represented 100% leakage.

4.11 AO/EB Double Staining Assay

MCF-7/PTX cells was used for AO/EB double staining. Briefly, MCF-7/PTX cells were grown in a 24-well plate at 5×10^4 cells per well, cultured for 24 h. Then the cells were treated with various concentration of conjugates for 12 h, respectively. Next, the cells were stained with 20 $\mu\text{g/ml}$ of AO/EB solution in the dark for 10 min. Subsequently, excess AO/EB dye mixture was washed with cold PBS. Fluorescence images were obtained with fluorescence microscopy (Nikon Ts2R).

4.12 Analysis of cell apoptosis

The reported procedures with minor modification was employed for the detection of percentage of apoptotic cells³⁸. In brief, apoptotic cells were quantitated by flow cytometry with annexin V-FITC/PI Detection Kit (Nanjing Jiancheng Bioengineering Institute). MCF-7/PTX cells were seeded in a 6-well plate and cultured overnight. Next, the cells were incubated with different concentrations of conjugates, or vehicle for 12 h and were later processed according to the manufacturer's instructions, and then, analyzed using the flow cytometer. (Beckman Coulter Accuri C6).

4.13 Cellular Colocalization.

Mitochondrial membrane potential was used to determine the influence of

compounds FA-P3-PTX and FA-P7-PTX on mitochondrial membrane, relying on the change of dye JC-1 red to green⁴⁴. Concisely, MCF-7/PTX cells were seeded in 6×10^4 cells in glass bottom cell culture dishes and incubated overnight and then treated with 3 μ M of PTX, FA-P3-PTX and FA-P7-PTX for 12 h and stained with JC-1 according to the protocol of Mitochondrial Membrane Potential Assay Kit (Beyotime Biotechnology). The change of fluorescence was visualized using confocal microscopy (Olympus IX81).

4.14 Western Blot Analysis of Caspase-3, Cytochrome-C and Folate receptor.

The western blot procedure was conducted based on the protocol reported formerly⁴³. MCF-7/PTX cells were seeded in a 10 cm dish. The cells were then treated with 3 μ M of FA-P3-PTX or FA-P7-PTX for 2 h. The mediums containing conjugates was discarded, and the cells were washed with cold PBS three times. Cellular proteins were extracted in the RIPA lysis buffer (Beyotime) containing 1 mM PMSF. The cell lysate was boiled in loading buffer for 10 min, and protein concentration was quantified by BCA method following the procedures of the kit. 40 μ g of cell lysate was resolved on gradient Bis-Tris acrylamide gels, and then transferred to PVDF membrane which were then blocked by incubation for 2 h at room temperature with 5% bovine serum albumin (BSA) in TBST buffer (10 mM Tris-HCl, pH 7.6, 150 mM NaCl, and 0.1% Tween 20) to block nonspecific binding. Subsequently, the membranes were incubated with primary antibodies (CASP3 antibody, CYCS antibody, folate receptor antibody and GADPH antibody) at 4 °C overnight. Next, the PVDF membranes were washed three times with TBST buffer and incubated with HRP-conjugated secondary antibody at room temperature for 2 h. After washing three times, the protein bands were displayed using Tanon High sig ECL western blotting and a luminescent image analyzer (Tanon 5500). GADPH was used to confirm equal loading in each lane in the samples prepared from cell lysates.

4.15 Tubulin Polymerization Assay

BK011P-Tubulin Polymerization Assay Kit was used to determine that compounds influence on Tubulin Polymerization. Briefly, tubulin (2 mg/mL) in buffer complement with 1mMGTP and 15% glycerol was utilized. Then, PTX and FA-P7-PTX were tested at 3 μ M final concentration (n = 3 replicates, single preparation). The changes in the fluorescence intensity (λ_{ex} =370 nm, λ_{em} = 445 nm) were tested by kinetic reading at 37°C using a PerkinElmer EnSpire multimode plate reader.

4.16 *In vitro* plasma stability

The stability of the conjugates was examined in plasma collected from Wistar rats, as previously described⁴⁹. Compounds were measured using an initial concentration of 500 ug/mL in rat plasma at 37 °C. At 0.5, 1, 2, 3, 4, 8, 12 and 24 h time points, 100 uL of mixture was extracted and then 400 uL of acetonitrile was added. After vortex, the mixture was centrifuged at 10000 \times g and supernatant were collected and analyzed using UPLC/MS.

4.17 Animal Model

ICR mice (male, 18–22 g, Certificate number: NO.201822692) were purchased from the Comparative Medical Center of Yangzhou University (Jiangsu, China). All the animals involved were treated in accordance with protocols approved by the ethical committee of China Pharmaceutical University. All animal experimental protocols adhered to the Guide for the Care and Use of Laboratory Animals published by the National Institutes of Health (NIH publication 85-23, revised 1986). H22 cells (5×10^6 cells/ml) were inoculated into the abdomen of male ICR mice, after 1 week,

the ascites was collected and diluted with 0.9% saline solution; the cell concentration was adjusted to 1×10^6 cells/ml and injected into each mice. After 6 days, the size of the tumors reached approximately $650\text{--}750\text{mm}^3$. 30 mice were randomly divided into three groups (ten mice per group) and subcutaneously administrated with 0.9% saline solution (control), PTX ((12 $\mu\text{mol/kg}$)) and FA-P7-PTX ((12 $\mu\text{mol/kg}$)). The mice were treated with compounds or saline once a day via peritumoral injection. Tumor size was monitored and measured by caliper measurements over a period of 22 days. The volume was calculated using the formula: tumor volume = $1/2ab^2$ (where a is the largest length and b is the smallest width). After the mouse were sacrificed, necropsies were performed and the tumors were removed, weighed.

4.18 Statistical analysis

Data were calculated using Microsoft Excel 2007 and/or GraphPad Prism 7.0. Data were presented as mean \pm SD for three independent tests. Comparisons among groups were statistically analyzed by one-way analysis of variance (ANOVA). P values <0.05 were considered significant.

Acknowledgements

This work was supported by the National Natural Science Foundation of China (No. 81872733 & No. 81673299).

Conflict of interest

The authors have no conflicts of interest to declare.

Appendix A. Supplementary material

Reference

- [1]. Bray, F.; Ferlay, J.; Soerjomataram, I.; Siegel, R. L.; Torre, L. A.; Jemal, A., Global cancer statistics 2018: GLOBOCAN estimates of incidence and mortality worldwide for 36 cancers in 185 countries. *Ca-a Cancer Journal for Clinicians* 2018, 68 (6), 394-424.
- [2]. Gottesman, M. M.; Fojo, T.; Bates, S. E., Multidrug resistance in cancer: Role of ATP-dependent transporters. *Nature Reviews Cancer* 2002, 2 (1), 48-58.
- [3]. Qiong, W.; Zhiping, Y.; Yongzhan, N.; Yongquan, S.; Daiming, F., Multi-drug resistance in cancer chemotherapeutics: mechanisms and lab approaches. *Cancer Letters* 2014, 347 (2), 159-166.
- [4]. Waghay, D.; Zhang, Q., Inhibit or Evade Multidrug Resistance P-Glycoprotein in Cancer Treatment. *Journal of Medicinal Chemistry* 2018, 61 (12), 5108-5121.
- [5]. Waghary, D.; Zhang, Q., Inhibit or Evade Multidrug Resistance P-Glycoprotein in Cancer Treatment. *Journal of Medicinal Chemistry* 2017.
- [6]. Schiff, P. B.; Fant, J., ; Horwitz, S. B., Promotion of microtubule assembly in vitro by taxol. *Nature* 1979, 277 (5698), 665.
- [7]. Hui, X.; Noah, D.; Huiying, S.; Haiyuan, Z.; Fangfang, F.; Jiawei, L.; Xuelian, N.; Shaochun, D.; Baogang, L.; Min, G., Proteomic Profiling of Paclitaxel Treated Cells Identifies a Novel Mechanism of Drug Resistance Mediated by PDCD4. *J. Proteome Res.* 2015, 14 (6), 2480.
- [8]. Li, F.; Lu, J.; Liu, J.; Liang, C.; Wang, M.; Wang, L.; Li, D.; Yao, H.; Zhang, Q.; Wen, J., A water-soluble nucleolin aptamer-paclitaxel conjugate for tumor-specific targeting in ovarian cancer. *Nature Communications* 2017, 8 (1), 1390.
- [9]. Yang, L.; Huang, L.; Feng, L., Paclitaxel Nanocrystals for Overcoming Multidrug Resistance in Cancer. *Mol. Pharm.* 2010, 7 (3), 863.
- [10]. Alqahtani, S. D.; Assiri, H. A.; Al-Abbasi, F. A.; El-Halawany, A. M.; Al-Abd, A. M., Rubrofusarin and toralactone sensitize resistant MCF-7(adr) cell line to paclitaxel via inhibiting P-glycoprotein efflux activity. *Cancer Research* 2017, 77.
- [11]. Duan, Z.; Chen, C.; Qin, J.; Liu, Q.; Wang, Q.; Xu, X.; Wang, J., Cell-penetrating peptide conjugates to enhance the antitumor effect of paclitaxel on drug-resistant lung cancer. *Drug Delivery* 2017, 24 (1), 752.
- [12]. Xie, X.; Shao, X.; Ma, W.; Zhao, D.; Shi, S.; Li, Q.; Lin, Y., Overcoming drug-resistant lung cancer by paclitaxel loaded tetrahedral DNA nanostructures. *Nanoscale* 2018, 10 (4), 10.1039.C7NR09692E.
- [13]. Sparreboom, A., ; Zuylen, L., Van; Brouwer, E., ; Loos, W. J.; Bruijn, P., De; Gelderblom, H., ; Pillay, M., ; Nooter, K., ; Stoter, G., ; Verweij, J., . Cremophor EL-mediated alteration of paclitaxel distribution in human blood: clinical pharmacokinetic implications. *Cancer Research* 1999, 59 (7), 1454-1457.

- [14]. Hennenfent, K. L.; Govindan, R., Novel formulations of taxanes: a review. Old wine in a new bottle? *Annals of Oncology* 2006, 17 (5), 735-749.
- [15]. Green, M. R.; Manikhas, G. S.; Afanasyev, B.; Makhson, A. M.; Bhar, P.; Hawkins, M. J., Abraxane, a novel Cremophor-free, albumin-bound particle form of paclitaxel for the treatment of advanced non-small-cell lung cancer. *Annals of Oncology* 2006, 17 (8), 1263-1268.
- [16]. Lee, K. S.; Chung, H. C.; Im, S. A.; Park, Y. H.; Kim, C. S.; Kim, S. B.; Sun, Y. R.; Min, Y. L.; Ro, J., Multicenter phase II trial of Genexol-PM, a Cremophor-free, polymeric micelle formulation of paclitaxel, in patients with metastatic breast cancer. *Breast Cancer Research & Treatment* 2008, 108 (2), 241-50.
- [17]. Lee, S. W.; Kim, Y. M.; Cho, C. H.; Kim, Y. T.; Kim, S. M.; Hur, S. Y.; Kim, J. H.; Kim, B. G.; Kim, S. C.; Ryu, H. S., An Open-Label, Randomized, Parallel, Phase II Trial to Evaluate the Efficacy and Safety of a Cremophor-Free Polymeric Micelle Formulation of Paclitaxel as First-Line Treatment for Ovarian Cancer: a Korean Gynecologic Oncology Group study (KGOG-3021). *Cancer Research & Treatment* 2018, 50 (1), 195-203.
- [18]. Kato, K.; Yoshikawa, T.; Yamaguchi, K.; Tsuji, Y.; Esaki, T.; Sakai, K.; Kimura, M.; Hamaguchi, T.; Shimada, Y.; Matsumura, Y., Phase II study of NK105, a paclitaxel-incorporating micellar nanoparticle, for previously treated advanced or recurrent gastric cancer. *Investigational New Drugs* 2012, 30 (4), 1621-1627.
- [19]. Sonsoles, Dipeptidyl-Peptidase IV (DPP IV/CD26)-Activated Prodrugs: A Successful Strategy for Improving Water Solubility and Oral Bioavailability. *Current Medicinal Chemistry* 2015, 22 (8), -.
- [20]. Hung, K.-y.; Harris, P. W. R.; Desai, A.; Marshall, J. F.; Brimble, M. A., Structure-activity relationship study of the tumour-targeting peptide A20FMDV2 via modification of Lys16, Leu13, and N- and/or C-terminal functionality. *European Journal of Medicinal Chemistry* 2017, 136, 154-164.
- [21]. Cheng, H.; Zhu, J. Y.; Xu, X. D.; Qiu, W. X.; Lei, Q.; Han, K.; Cheng, Y. J.; Zhang, X. Z., Activable Cell-Penetrating Peptide Conjugated Prodrug for Tumor Targeted Drug Delivery. *Acs Applied Materials & Interfaces* 2015, 7 (29).
- [22]. Darwish, S.; Sadeghiani, N.; Fong, S.; Mozaffari, S.; Hamidi, P.; Withana, T.; Yang, S.; Tiwari, R. K.; Parang, K., Synthesis and antiproliferative activities of doxorubicin thiol conjugates and doxorubicin-SS-cyclic peptide. *European journal of medicinal chemistry* 2019, 161, 594-606.
- [23]. Dong, Y.; Wang, S. H.; Wang, C. T.; Li, Z. H.; Ma, Y.; Liu, G., Antagonizing NOD2 Signaling with Conjugates of Paclitaxel and Muramyl Dipeptide Derivatives Sensitizes Paclitaxel Therapy and Significantly Prevents Tumor Metastasis. *Journal of Medicinal Chemistry* 2017, 60 (3), 1219-1224.
- [24]. Ma, Y.; Zhao, N.; Liu, G., Conjugate (MTC-220) of Muramyl Dipeptide Analogue and Paclitaxel Prevents Both Tumor Growth and Metastasis in Mice. *Journal of Medicinal Chemistry* 2011, 54 (8), 2767-2777.
- [25]. Yuan, S.; You, Y.; Yun, C., Dual-targeting hybrid peptide-conjugated doxorubicin for drug resistance reversal in breast cancer. *International Journal of Pharmaceutics* 2016, 512 (1), 1-13.
- [26]. Zasloff, M., Antimicrobial peptides of multicellular organisms. *Nature* 2002, 415 (6870), 389-395.
- [27]. Liu, X.; Cao, R.; Wang, S.; Jia, J.; Fei, H., Amphipathicity determines different cytotoxic mechanisms of lysine- or arginine-rich cationic hydrophobic peptides in cancer cells. *Journal of Medicinal Chemistry* 2016, 59 (11), 5238.
- [28]. WC, W., Describing the mechanism of antimicrobial peptide action with the interfacial activity model. *Acs Chemical Biology* 2010, 5 (10), 905.

- [29]. Claudio Borges, F.; Clara, P. P.; Torre, B. G., De La; Xavier, M.; Héctor, Z. C.; M Ángeles, J.; Gandhi, R. B.; David, A., Structural Dissection of Crotalicidin, a Rattlesnake Venom Cathelicidin, Retrieves a Fragment with Antimicrobial and Antitumor Activity. *Journal of Medicinal Chemistry* 2015, 58 (21), 8553-8563.
- [30]. Xia, W.; Low, P. S., Folate-Targeted Therapies for Cancer. *Journal of Medicinal Chemistry* 2010, 53 (19), 6811-6824.
- [31]. Cao, Y.; Yang, J., Development of a folate receptor (FR)-targeted indenoisoquinoline using a pH-sensitive N-ethoxybenzylimidazole (NEBI) bifunctional cross-linker. *Bioconjugate Chem.* 2014, 25 (5), 873.
- [32]. Adrian, S.; Justin, L.; Anton, B.; Bongiovanni, M. N.; Lydia, O.; Gras, S. L.; Xiaoqing, Z.; Qiao, G. G., Folic acid conjugated amino acid-based star polymers for active targeting of cancer cells. *Biomacromolecules* 2011, 12 (10), 3469-77.
- [33]. Chuanqiang, N.; Qiquan, S.; Jingxing, Z.; Du, C.; Guobin, H., Folate-functionalized polymeric micelles based on biodegradable PEG-PDLLA as a hepatic carcinoma-targeting delivery system. *Asian Pac. J. Cancer Prev.* 2011, 12 (8), 1995-1999.
- [34]. Gaspar, V. M.; Costa, E. C.; Queiroz, J. A.; Pichon, C.; Sousa, F.; Correia, I. J., Folate-Targeted Multifunctional Amino Acid-Chitosan Nanoparticles for Improved Cancer Therapy. *Pharmaceutical Research* 2015, 32 (2), 562-577.
- [35]. Wang, X.; Li, J.; Wang, Y.; Koenig, L.; Gjyzezi, A.; Giannakakou, P.; Shin, E. H.; Tighiouart, M.; Chen, Z.; Nie, S.; Shin, D. M., A Folate Receptor-Targeting Nanoparticle Minimizes Drug Resistance in a Human Cancer Model. *Acs Nano* 2011, 5 (8), 6184-6194.
- [36]. Naumann, R. W.; Coleman, R. L.; Burger, R. A.; Sausville, E. A.; Kutarska, E.; Ghamande, S. A.; Gabrail, N. Y.; DePasquale, S. E.; Nowara, E.; Gilbert, L.; Gersh, R. H.; Teneriello, M. G.; Harb, W. A.; Konstantinopoulos, P. A.; Penson, R. T.; Symanowski, J. T.; Lovejoy, C. D.; Leaman, C. P.; Morgenstern, D. E.; Messmann, R. A., PRECEDENT: A Randomized Phase II Trial Comparing Vintafolide (EC145) and Pegylated Liposomal Doxorubicin (PLD) in Combination Versus PLD Alone in Patients With Platinum-Resistant Ovarian Cancer. *Journal of Clinical Oncology* 2013, 31 (35), 4400-+.
- [37]. Hanna, N.; Juhasz, E.; Cainip, C.; Gladkov, O.; Juan Vidal, O.; Ramlau, R.; Vidal, O. J.; Lal, R.; Symanowski, J.; Clark, R.; Harb, W., A Randomized Phase 2 Trial of Vintafolide and Docetaxel in Folate-Receptor Positive (FR plus) Advanced NSCLC Patients: Final Efficacy Results. *Journal of Thoracic Oncology* 2015, 10 (9), S173-S173.
- [38]. Dai, Y.; Cai, X.; Wei, S.; Bi, X.; Xin, S.; Pan, M.; Li, H.; Lin, H.; Huang, W.; Hai, Q., Pro-apoptotic cationic host defense peptides rich in lysine or arginine to reverse drug resistance by disrupting tumor cell membrane. *Amino Acids* 2017, 49 (8).
- [39]. Jie, Z.; Cai, X.; Xun, H.; Dai, Y.; Sun, L.; Bo, Z.; Bo, Y.; Lin, H.; Huang, W.; Hai, Q., A novel glucagon-like peptide-1/glucagon receptor dual agonist exhibits weight-lowering and diabetes-protective effects. *European Journal of Medicinal Chemistry* 2017, 138, 1158-1169.
- [40]. Deng, X.; Qiu, Q.; Yang, B.; Wang, X.; Huang, W.; Qian, H., Design, synthesis and biological evaluation of novel peptides with anti-cancer and drug resistance-reversing activities. *European Journal of Medicinal Chemistry* 2015, 89 (3), 540-548.
- [41]. Untereiner, A. A.; Oláh, G.; Módis, K.; Hellmich, M. R.; Szabo, C., H₂S-induced S-sulfhydration of lactate dehydrogenase a (LDHA) stimulates cellular bioenergetics in HCT116 colon cancer cells. *Biochemical Pharmacology* 2017, 136, 86.

- [42]. Aitken, R. J.; Muscio, L.; Whiting, S.; Connaughton, H. S.; Fraser, B. A.; Nixon, B.; Smith, N. D.; Iuliis, G. N. D., Analysis of the effects of polyphenols on human spermatozoa reveals unexpected impacts on mitochondrial membrane potential, oxidative stress and DNA integrity; implications for assisted reproductive technology. *Biochemical Pharmacology* 2016, 121.
- [43]. Yamaguchi, T.; Hashiguchi, K.; Katsuki, S.; Iwamoto, W.; Tsuruhara, S.; Terada, S., Activation of the intrinsic and extrinsic pathways in high pressure-induced apoptosis of murine erythroleukemia cells. *Cellular & Molecular Biology Letters* 2008, 13 (1), 49-57.
- [44]. Perelman, A.; Wachtel, C.; Cohen, M.; Haupt, S.; Shapiro, H.; Tzur, A., JC-1: alternative excitation wavelengths facilitate mitochondrial membrane potential cytometry. *Cell Death & Disease* 2012, 3 (11), e430.
- [45]. Furre, I. E.; Shahzidi, S.; Luksiene, Z.; Møller, M. T.; Borgen, E.; Morgan, J.; Tkacz-Stachowska, K.; Nesland, J. M.; Peng, Q., Targeting PBR by hexaminolevulinate-mediated photodynamic therapy induces apoptosis through translocation of apoptosis-inducing factor in human leukemia cells. *Cancer Research* 2013, 65 (23), 11051-11060.
- [46]. Kuida, K., .; Haydar, T. F.; Kuan, C. Y.; Gu, Y., .; Taya, C., .; Karasuyama, H., .; Su, M. S.; Rakic, P., .; Flavell, R. A., Reduced apoptosis and cytochrome c-mediated caspase activation in mice lacking caspase 9. *Cell* 1998, 94 (3), 325-337.
- [47]. Jing, H.; Lidan, S.; Yingying, C.; Zheng, L.; Dandan, H.; Xiaoyun, Z.; Hai, Q.; Wenlong, H., Design, synthesis, and biological activity of novel dicoumarol glucagon-like peptide 1 conjugates. *Journal of Medicinal Chemistry* 2013, 56 (24), 9955-9968.
- [48]. Newcomb, C. J.; Sur, S.; Ortony, J. H.; Lee, O. S.; Matson, J. B.; Boekhoven, J.; Yu, J. M.; Schatz, G. C.; Stupp, S. I., Cell death versus cell survival instructed by supramolecular cohesion of nanostructures. *Nature Communications* 2014, 5, 3321.
- [49]. Soudy, R.; Chen, C.; Kaur, K., Novel Peptide-Doxorubicin Conjugates for Targeting Breast Cancer Cells Including the Multidrug Resistant Cells. *Journal of Medicinal Chemistry* 2013, 56 (19), 7564-7573.

Highlights

- Synthesis of folic acid-peptide- paclitaxel conjugates.
- FA-P7-PTX possessed high potency in drug resistant cancer cells MCF-7/PTX with IC_{50} of 2.92 ± 0.2 μ M.
- FA-P7-PTX exhibited membrane disrupting and pro-apoptosis activity and tumor growth inhibitory activities *in vivo*.
- FA-P7-PTX shown induction of a mitochondrial impairment and caspase-3-dependent apoptotic cell death.
- All results indicated FA-P7-PTX was a potential candidate for drug resistant cancer therapy deserving further study.